An *Encephalitozoon cuniculi* Ortholog of the RNA Polymerase II Carboxyl-Terminal Domain (CTD) Serine Phosphatase Fcp1[†]

Stéphane Hausmann,[‡] Beate Schwer,[§] and Stewart Shuman*,[‡]

Molecular Biology Program, Sloan-Kettering Institute, New York, New York 10021, and Microbiology and Immunology Department, Weill Medical College of Cornell University, New York, New York 10021

Received January 5, 2004; Revised Manuscript Received April 7, 2004

ABSTRACT: Fcp1 is an essential protein serine phosphatase that dephosphorylates Ser2 or Ser5 of the RNA polymerase II carboxyl-terminal domain (CTD) heptad repeat $Y^1S^2P^3T^4S^5P^6S^7$. The CTD of the microsporidian parasite *Encephalitozoon cuniculi* consists of 15 heptad repeats, which approximates the minimal CTD length requirement for cell viability in yeast. Here we show that *E. cuniculi* encodes a minimized 411-aa Fcp1-like protein (EcFcp1), which consists of a DxDx(T/V) phosphatase domain and a BRCA1 carboxyl terminus (BRCT) domain but lacks the large N- and C-terminal domains found in fungal and metazoan Fcp1 enzymes. Nonetheless, EcFcp1 can function in lieu of *Saccharomyces cerevisiae* Fcp1 to sustain yeast cell growth. Recombinant EcFcp1 is a monomeric enzyme with intrinsic phosphatase activity against nonspecific (*p*-nitrophenyl phosphate) and specific (CTD-PO_4) substrates. EcFcp1 dephosphorylates CTD positions Ser2 and Ser5 with similar efficacy in vitro. We exploit synthetic CTD Ser2-PO_4 and Ser5-PO_4 peptides to define minimized substrates for EcFcp1 and to illuminate the importance of CTD primary structure in Ser2 and Ser5 phosphatase activity.

The carboxyl-terminal domain (CTD)[1] of the largest subunit of RNA polymerase II (Pol II) is composed of a tandemly repeated heptapeptide of consensus sequence $Y^1S^2P^3T^4S^5P^6S^7$. The number of CTD heptad repeats varies widely among species and correlates roughly with evolutionary complexity, for example, mammals have 52 repeats, *Drosophila melanogaster* has 42 repeats, and fission yeast has 29 repeats. Deletion analyses of the Pol II large subunit have shown that cell growth is contingent on a minimal CTD length. Mammalian cells cannot grow with 25 or fewer CTD heptad repeats but are viable with 36 repeats (*1*). *Drosophila melanogaster* is inviable when the CTD is truncated to 20 heptad repeats (*2*). The threshold is lower in *Saccharomyces cerevisiae*, where less than 8 heptad repeats are lethal, 8 to 10 repeats result in conditional growth phenotypes, and 11 or more repeats suffice for apparently normal growth (*3, 4*).

The microsporidian parasite *Encephalitozoon cuniculi* has the smallest genome (∼2.9 Mbp; ∼2000 protein-encoding genes) of any known eukaryote (*5*). The coding density of the *E. cuniculi* genome is exceptionally high, and it has been suggested that this organism generally produces smaller versions of protein counterparts encoded by organisms with much larger genomes (*5*). In this light, it is notable that the *E. cuniculi* Pol II CTD (Genbank accession CAD26175) consists of only 15 tandem heptad repeats, 14 of which conform precisely to the $Y^1S^2P^3T^4S^5P^6S^7$ consensus sequence.

CTD positions Ser5 and Ser2 undergo waves of phosphorylation and dephosphorylation during the transcription cycle. Remodeling of the CTD phosphorylation array accompanies the transition from initiation to elongation modes and controls the recruitment, activity, and egress of the various mRNA processing machines that act on the nascent transcript (*6*−*8*). Knowledge of the atomic structure of the phosphorylated CTD and how such parameters as CTD length, amino acid sequence, and phosphorylation arrays influence CTD-PO_4 effector functions has emerged from studies of the interaction of mRNA capping enzymes with the phosphorylated CTD (*9*−*11*). An initial characterization of the triphosphatase, guanylyltransferase, and guanine-N7 methyltransferase components of the *E. cuniculi* capping apparatus revealed that these enzymes have been pared down in size relative to their orthologs from other eukarya to the point that they consist of little more than the minimum catalytic domains (*12*). This natural minimization proved advantageous for structural analysis of the *E. cuniculi* cap methyltransferase (*13*), which, like its yeast ortholog, can bind directly to the phosphorylated CTD.

Eukaryotic cells contain multiple protein serine kinases (*14*) and protein serine phosphatases (*15*−*17*) that modify the CTD. Among the CTD phosphatases, Fcp1 has been studied most intensively. Fcp1, which was initially isolated from human cells by Dahmus and colleagues (*18*), is the major protein serine phosphatase responsible for removing phosphates from the CTD (*18*−*27*). Fcp1 is essential for cell viability in budding and fission yeast (*20, 26*). A partial deficiency of human Fcp1 is associated with the autosomal recessive developmental disorder characterized by cataracts, facial dysmorphism, and peripheral neuropathy (*28*).

[†] Supported by NIH Grant GM52470.

* Corresponding author. Phone: (212) 639−7145. Fax: (212) 717−3623. E-mail: s-shuman@ski.mskcc.org.

[‡] Sloan-Kettering Institute.

[§] Weill Medical College of Cornell University.

[1] Abbreviations: CTD, carboxyl-terminal domain; Pol II, RNA polymerase II; FCPH, FCP1 homology; BRCT, BRCA1 carboxyl terminus.

10.1021/bi0499617 CCC: $27.50
Published on Web 05/08/2004

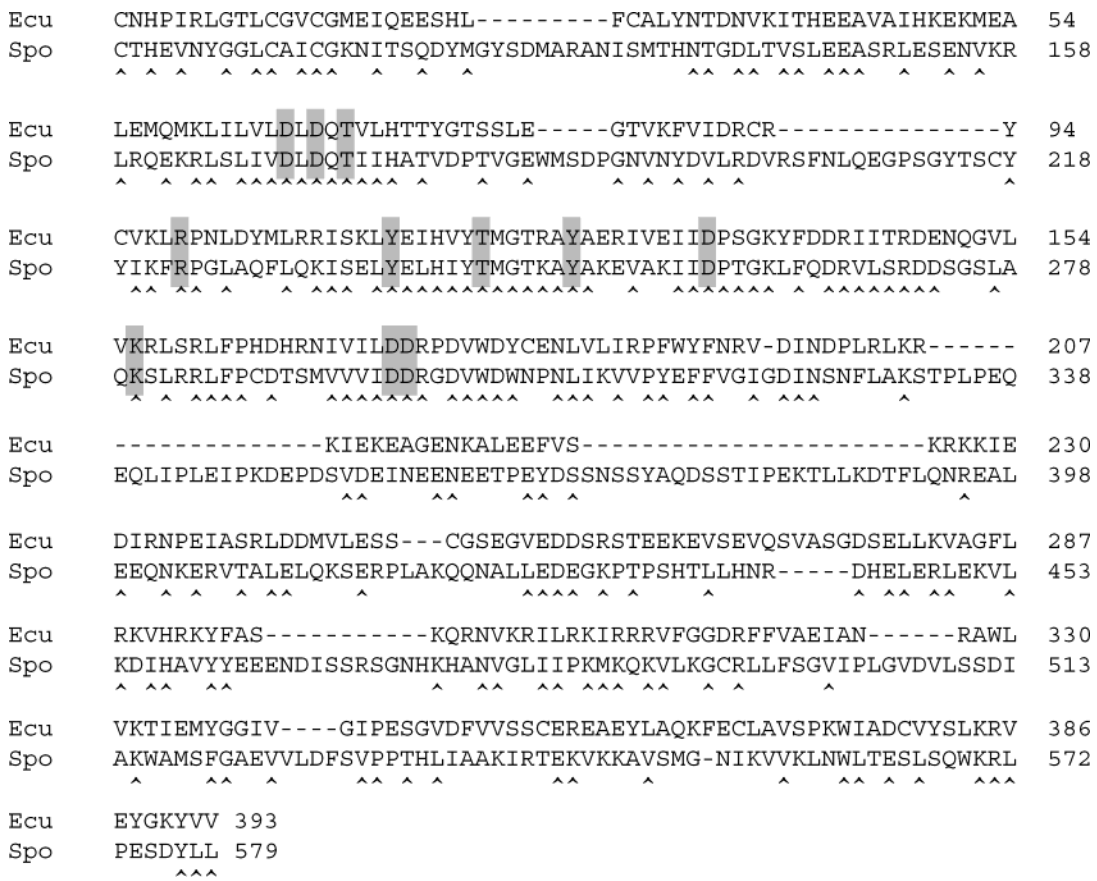

FIGURE 1: An *E. cuniculi* homologue of *Sc. pombe* Fcp1. The amino acid sequence of *E. cuniculi* (Ecu) Fcp1 from residues 4 to 393 is aligned to the sequences of *Sc. pombe* (Spo) Fcp1 from residues 99 to 579. Gaps in the alignment are indicated by dashes. Positions of side chain identity/similarity are indicated by ∧. The 11 residues of *Sc. pombe* Fcp1 that were defined by mutational analysis as essential for phosphatase activity are highlighted in shaded boxes.

Fcp1 orthologs are relatively large polypeptides (723-aa in *Schizosaccharomyces pombe*; 732-aa in *S. cerevisiae*; 961-aa in humans) consisting of a conserved central catalytic domain flanked by variable N- and C-terminal segments that are dispensable for CTD phosphatase activity in vitro (*27, 29*) but are collectively required for *S. cerevisiae* Fcp1 function in vivo (*30*). The minimal phosphatase domain of *Sc. pombe* Fcp1 is a 425-aa polypeptide spanning residues 156−580 (*29*). The catalytic domain is itself composed of two modules: an N-terminal FCPH (FCP1 homology) domain spanning *Sc. pombe* Fcp1 residues 140−326 (Figure 1) and a C-terminal BRCT (BRCA1 carboxyl terminus) domain, both of which are essential for Fcp1 phosphatase activity in vivo and in vitro (*24, 27, 30*). The FCPH domain of Fcp1 belongs to the DxDx(T/V) family of metal-dependent phosphotransferases that act via an acyl-phosphoenzyme intermediate (*31*). Mutational analysis of the FCPH domain of *Sc. pombe* Fcp1 identified a constellation of 11 essential amino acids (highlighted in boxes in Figure 1) that are conserved in other Fcp1 orthologs and likely comprise the active site (*27, 29, 32*). The BRCT domain is implicated in recognition of the CTD-PO_4 substrate (*33*).

To gain insight to the evolution of the network of CTD modification enzymes, we sought to identify a CTD phosphatase ortholog in the "minimal" proteome of *E. cuniculi*. A psi-blast search using the 723-aa *Sc. pombe* Fcp1 (hereafter SpFcp1) revealed a 411-aa *E. cuniculi* polypeptide that contains putative homologues of the FCPH and BRCT domains of ScFcp1 but lacks the flanking N- and C-terminal segments (Figure 1). An alignment of the *Sc. pombe* and *E. cuniculi* polypeptides highlights 190 positions of side chains identity/similarity, including strict conservation of all of the 11 residues of the FCPH domain found to be essential for the phosphatase activity of SpFcp1 (Figure 1). Here we address several key questions concerning this putative microsporidian Fcp1 (referred to hereafter as EcFcp1). Is EcFcp1 a bona fide CTD phosphatase? Does it have a preference for dephosphorylation of Ser2 versus Ser5? How does CTD primary structure dictate EcFcp1 phosphatase activity? Is EcFcp1 a true functional ortholog of yeast Fcp1 in vivo?

EXPERIMENTAL PROCEDURES

Recombinant EcFcp1. The *EcFCP1* coding sequence (Genbank accession AL590447) was PCR-amplified from *E. cuniculi* genomic DNA (obtained from Dr. Christian Vivarès) using primers designed to introduce an *Nco*I site at the translation start codon and an *Xho*I site 3′ of the translation stop codon. The PCR product was digested with *Nco*I and *Xho*I and then inserted between the *Nco*I and *Xho*I sites of the yeast vector pYX232 (2μ *TRP1*). Sequencing of the *EcFCP1* insert and comparison to the sequence in Genbank confirmed that no coding changes were introduced during amplification and cloning. The EcFCP1 coding sequence was excised from pYX-EcFCP1 with *Nco*I and *Xho*I and the 5′ overhangs were filled in using T4 DNA polymerase. The blunt DNA fragment was inserted into pET28-His_{10}-Smt3 that had been linearized with *Bam*HI and

filled-in using T4 DNA polymerase. The resulting expression plasmid pET-His_{10}-Smt3-EcFcp1 encodes EcFcp1 fused in-frame to an N-terminal His_{10}-Smt3 domain consisting of a His_{10} leader peptide (MGHHHHHHHHHHSSGHIEGRH) followed by the 98-aa *S. cerevisiae* Smt3 protein and a single serine. (Smt3 is the yeast ortholog of the small ubiquitin-like modifier SUMO.) pET-His_{10}-Smt3-EcFcp1 was transformed into *Escherichia coli* BL21(DE3)-RIL (Stratagene). A 500-mL culture derived from a single transformant was grown at 37 °C in LB medium containing 50 μg/mL kanamycin and 50 μg/mL chloramphenicol until the A_{600} reached 0.6. The culture was adjusted to 0.2 mM IPTG and 2% ethanol, and incubation was continued for 20 h at 17 °C. Cells were harvested by centrifugation and stored at −80 °C. All subsequent procedures were performed at 4 °C. Thawed bacteria were resuspended in 25 mL of buffer A (50 mM Tris-HCl, pH 8.0, 200 mM NaCl, 10% glycerol). Phenylmethylsulfonyl Fluoride (PMSF) and lysozyme were added to final concentrations of 500 μM and 100 μg/mL, respectively. After incubation on ice for 30 min, Triton X-100 was added to a final concentration of 0.1%, and the lysate was sonicated to reduce viscosity. Insoluble material was removed by centrifugation for 1 h at 18 000 rpm in a Sorvall SS34 rotor. The soluble extract was mixed for 30 min with 1 mL of Ni^{2+}−NTA−agarose (Qiagen) that had been equilibrated with buffer A containing 0.1% Triton X-100. The column was washed with 10 mL of the same buffer and then eluted stepwise with 2.5 mL aliquots of buffer B (50 mM Tris-HCl, pH 8.0, 0.2 M NaCl, 10% glycerol, 0.1% Triton X-100) containing 50, 100, 250, and 500 mM imidazole. The polypeptide compositions of the column fractions were monitored by SDS−PAGE. The recombinant His_{10}-Smt3-EcFcp1 polypeptide was recovered predominantly in the 250 and 500 mM imidazole fractions. The 250 mM imidazole eluate was dialyzed against buffer containing 50 mM Tris-HCl (pH 7.5), 200 mM NaCl, 1 mM DTT, 10% glycerol, and 0.01% Triton X-100 and stored at −80 °C. The protein concentration was determined by SDS−PAGE analysis of serial dilutions of the EcFcp1 preparation in parallel with serial dilutions of a BSA standard. The gels were stained with Coomassie Blue, and the staining intensities of the His_{10}-Smt3-EcFcp1 and BSA polypeptides were quantified using a Fujifilm FLA-5000 digital imaging and analysis system.

Removal of the His_{10}-Smt3 Tag. An aliquot of the dialyzed Ni−agarose fraction of His_{10}-Smt3-EcFcp1 (100 μg) was treated for 1 h on ice with purified recombinant His-tagged *S. cerevisiae* Ulp1, a Smt3-specific cysteine protease (*34*), at a 1/40 ratio of Ulp1 to His_{10}-Smt3-EcFcp1. The digest was then applied to 0.5-mL column of Ni^{2+}−NTA−agarose to adsorb the cleaved His_{10}-Smt3 domain. The Ni−agarose flow-though fraction containing native EcFcp1 was stored at −80 °C.

Velocity Sedimentation. An aliquot (40 μg) of the native EcFcp1 preparation was mixed with catalase (40 μg), BSA (40 μg), and cytochrome *c* (40 μg), and the mixture was applied to a 4.8-mL 15−30% glycerol gradient containing 50 mM Tris-HCl (pH 7.4), 0.2 M NaCl, 1 mM EDTA, 2 mM DTT, 0.05% Triton X-100. The gradient was centrifuged in a SW50 rotor at 50 000 rpm for 15 h at 4 °C. Fractions (0.18 mL) were collected from the bottom of the tube. Aliquots (20 μL) of odd-numbered gradient fractions were analyzed by SDS−PAGE. Aliquots (20 μL) of every fraction were assayed for hydrolysis of *p*-nitrophenyl phosphate (pNØP).

Phosphatase Assay. Reaction mixtures (200 μL) containing 50 mM Tris-acetate (pH 6.5), 10 mM $MgCl_2$, 10 mM pNØP, and EcFcp1 as specified were incubated for 1 h at 37 °C. The reactions were quenched by adding 1 mL of 1 M sodium carbonate. Release of *p*-nitrophenol (pNØ) was determined by measuring A_{410} and interpolating the value to a pNØ standard curve.

CTD Phosphopeptides. CTD Ser-PO_4 peptides containing an unmodified N-terminal amine and a C-terminal acid were synthesized and purified by the Sloan-Kettering Microchemistry Core Laboratory as described previously (*9, 10, 32*). The peptides were dissolved in 10 mM Tris-HCl (pH 7.4) and 1 mM EDTA and stored at 4 °C. The molar concentrations of the phosphopeptides were initially estimated from the absorbance at 274 nM using an extinction coefficient of 1.4×10^3 M^{-1} for tyrosine. The content of Ser-PO_4 was then determined for each peptide measuring the release of inorganic phosphate after digestion with calf intestinal phosphatase (CIP; purchased from Roche) as follows: CIP reaction mixtures (25 μL) containing 2.5−5 nmol of CTD phosphopeptide and CIP (2 units) were incubated for 60 min at 37 °C. The reactions were quenched by adding 0.5 mL of malachite green reagent (BIOMOL Research Laboratories, Plymouth Meeting, PA). Release of phosphate was determined by measuring A_{620} and interpolating the value to a phosphate standard curve. The phosphopeptide concentrations measured by CIP were in good agreement (±10%) with the concentrations calculated from the UV absorbance. The amounts of input CTD Ser-PO_4 substrate specified in the EcFcp1 reactions are based on the concentrations determined by CIP digestion.

CTD Phosphatase Assay. Reaction mixtures (25 μL) containing 50 mM Tris-acetate (pH 7.0), 10 mM $MgCl_2$, CTD phosphopeptide, and EcFcp1 were incubated for 60 min at 37 °C. The reactions were quenched by adding 0.5 mL of malachite green reagent. Release of phosphate was determined by measuring A_{620} and interpolating the value to a phosphate standard curve.

Deletion of FCP1 in S. cerevisiae. The *FCP1* open reading frame encoding amino acids 221−625 of the 733-aa *S. cerevisiae* Fcp1 polypeptide was deleted in the *S. cerevisiae* diploid strain W303 and replaced with *LEU2* as follows. W303 was transformed with a linearized pUC-*fcp1::LEU2* cassette containing 1.4 kbp of yeast genomic DNA 5′ of the *FCP1* translation start codon and 1 kbp of DNA 3′ of the *FCP1* translation stop codon. Correct gene targeting was confirmed by Southern blotting of Leu^+ transformants. The *FCP1 fcp1::LEU2* diploid was sporulated, and tetrads were dissected. No viable Leu^+ haploids were derived from the diploid, indicative of *FCP1* being an essential gene, as reported previously (*20*). To obtain viable *fcp1*Δ haploids, an *FCP1 fcp1::LEU2* diploid was transformed with plasmid p360-FCP1 (*FCP1 URA3 CEN*). p360-FCP1 contains a restriction fragment of yeast genomic DNA extending from 791-bp upstream of the *FCP1* translation start codon to 751-bp downstream of the *FCP1* translation stop codon. The resulting Ura^+ diploid was sporulated and dissected. We thereby recovered viable *fcp1::LEU2* haploids that were unable to grow in the presence of 5-fluoroorotic acid (5-

FOA), a drug that selects against the *FCP1 URA3* plasmid.

Plasmid Shuffle Assay of EcFcp1 Function in Vivo. A *Mat***a** *fcp1*Δ p360-FCP1 strain was used to assay *fcp1*Δ complementation by plasmid shuffle. *fcp1*Δ cells were transformed with either p358-FCP1 (*FCP1 TRP1 CEN*), the parent vector pSE358 (*TRP1 CEN*), or one of the following yeast plasmids expressing EcFcp1: (i) pYX232-EcFCP1 (2*μ TRP1*), which expresses wild-type EcFcp1 under the transcriptional control of the yeast *TPI1* promoter, (ii) pYX232-D66A or pYX232-D68A (2*μ TRP1*), which express catalytically defective EcFcp1 mutants D66A or D68A under the control of the *TPI1* promoter; (iii) pYX132-EcFCP1 (*CEN TRP1*), which expresses wild-type EcFcp1 driven by yeast *TPI1* promoter. Trp^+ transformants were selected on medium lacking tryptophan. Two individual colonies were patched on Trp^- medium, and cells from each patch were then streaked on medium containing 0.75 mg/mL 5-FOA. The plates were incubated at 18, 25, 30, and 37 °C. The *CEN FCP1* and *2μ EcFCP1* plasmids supported colony formation within 4 days at 30 °C, whereas *fcp1*Δ cells expressing EcFcp1 mutants D66A or D68A failed to form colonies after 10 days at 18, 25, or 30 °C. Individual FOA-resistant isolates were streaked on yeast extract/peptone/dextrose (YPD) agar at 18, 25, 30, and 37 °C.

RESULTS

Phosphatase Activity of Recombinant E. cuniculi Fcp1. The open reading frame encoding EcFcp1 was cloned into a bacterial expression vector so as to fuse the EcFcp1 protein to an N-terminal His_{10}-Smt3 domain (*34*). The His_{10}-Smt3-EcFcp1 protein was purified from a soluble bacterial extract by adsorption to nickel−agarose and subsequent elution with buffer containing imidazole. SDS−PAGE analysis showed that the His_{10}-Smt3-EcFcp1 polypeptide was recovered in the 250 and 500 mM imidazole eluates (Figure 2A).

Initial detection of a generic phosphatase activity associated with the recombinant tagged EcFcp1 protein was achieved using 10 mM pNØP as a substrate. The *p*-nitrophenol (pNØ) reaction product was quantified via its absorbance at 410 nM. We found that His_{10}-Smt3-EcFcp1 catalyzed the conversion of pNØP to pNØ and that the extent of the reaction was directly proportional to the concentration of the recombinant protein (Figure 3A). His_{10}-Smt3-EcFcp1 released 19 nmol of pNØ per microgram of protein during a 60 min reaction, corresponding to a turnover number of 0.3 s^{-1}. Phosphatase activity was optimal at pH 6.0−8.5 (Figure 3B). Hydrolysis of pNØP by His_{10}-Smt3-EcFcp1 required a divalent cation cofactor. Magnesium supported optimal activity at 10 mM concentration (Figure 3C). Calcium was ineffective as a phosphatase cofactor up to 10 mM concentration (Figure 3C).

Sedimentation Analysis of Recombinant Native EcFcp1. The His_{10}-Smt3 domain was removed by treatment of the His_{10}-Smt3-EcFcp1 preparation with purified His_6-tagged Ulp1, a Smt3-specific protease that hydrolyzes the polypeptide chain at the junction between His_{10}-Smt3 and the fused downstream protein (*34*). SDS−PAGE analysis of the Ulp1-digested material showed that the original 66 kDa His_{10}-Smt3-EcFcp1 polypeptide was converted to a 50 kDa species corresponding to native EcFcp1 (Figure 2B). Note that the two principal contaminant polypeptides in the nickel−agarose

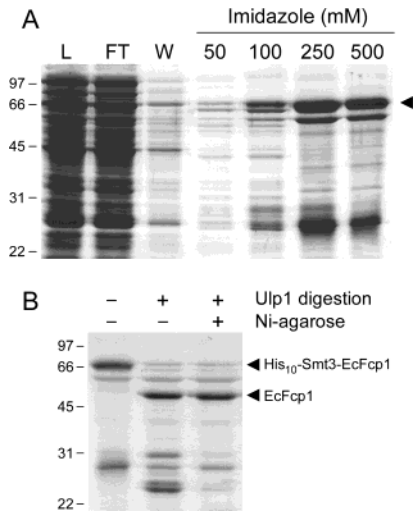

FIGURE 2: Recombinant His_{10}-Smt3-EcFcp1 and native EcFcp1 proteins. In panel A, His_{10}-Smt3-EcFcp1 was produced in *E. coli* and purified by nickel−agarose chromatography as described under Experimental Procedures. Aliquots (10 μL) of the soluble bacterial lysate (lane L), the nickel−agarose flow-through (lane FT), and wash (lane W) fractions and aliquots (20 μL) of the 50, 100, 250, and 500 mM imidazole eluate fractions were analyzed by SDS−PAGE. The polypeptides were visualized by staining the gel with Coomassie Blue dye. The positions and sizes (kDa) of marker polypeptides are indicated on the left. The position of the His_{10}-Smt3-EcFcp1 polypeptide is indicated by an arrowhead on the right. In panel B, digestion of His_{10}-Smt3-EcFcp1 (left lane) with Ulp1 yielded native EcFcp1 (middle lane), which was passed through a nickel-agarose column to remove the cleaved tag. The polypeptide composition of the nickel−agarose flow through fraction of native EcFcp1 is shown in the right lane. Aliquots (2 μg) of the protein preparations were analyzed by SDS−PAGE. The Coomassie Blue stained gel is shown.

protein preparation (migrating at ∼60 and ∼28 kDa) were not cleaved by Ulp1. The tag-free native EcFcp1 was fractionated away from the His_{10}-Smt3 fragment by nickel−agarose chromatography. SDS−PAGE analysis of the nickel−agarose flow-through fraction confirmed that the His_{10}-Smt3 fragment (migrating at ∼24 kDa) had been removed (Figure 2B). The native EcFcp1 preparation catalyzed magnesium-dependent hydrolysis of pNØP. Native EcFcp1 released 15 nmol of pNØ per microgram of protein during a 60 min reaction (data not shown), corresponding to a turnover number of 0.2 s^{-1} (similar to that of the His_{10}-Smt3-EcFcp1 fusion protein).

The quaternary structure of native recombinant EcFcp1 was investigated by zonal velocity sedimentation through a 15−30% glycerol gradient (Figure 4). Marker proteins catalase (native size 248 kDa), BSA (66 kDa), and cytochrome *c* (12 kDa) were included as internal standards in the gradient. After centrifugation, the polypeptide compositions of the odd-numbered gradient fractions were analyzed by SDS−PAGE. EcFcp1 (calculated to be a 48 kDa polypeptide) sedimented as a discrete peak nearly coincident with BSA. The phosphatase activity profile paralleled the abundance of the EcFcp1 polypeptide and peaked at fractions 20 and 21. A plot of the *S* values of the three standards versus fraction number yielded a straight line (not shown). An *S* value of 4.2 was determined for EcFcp1 by interpolation to the internal standard curve. These results are consistent with a monomeric quaternary structure for EcFcp1.

CTD Phosphatase Activity of EcFcp1. To gauge whether His_{10}-Smt3-EcFcp1 has CTD phosphatase activity and

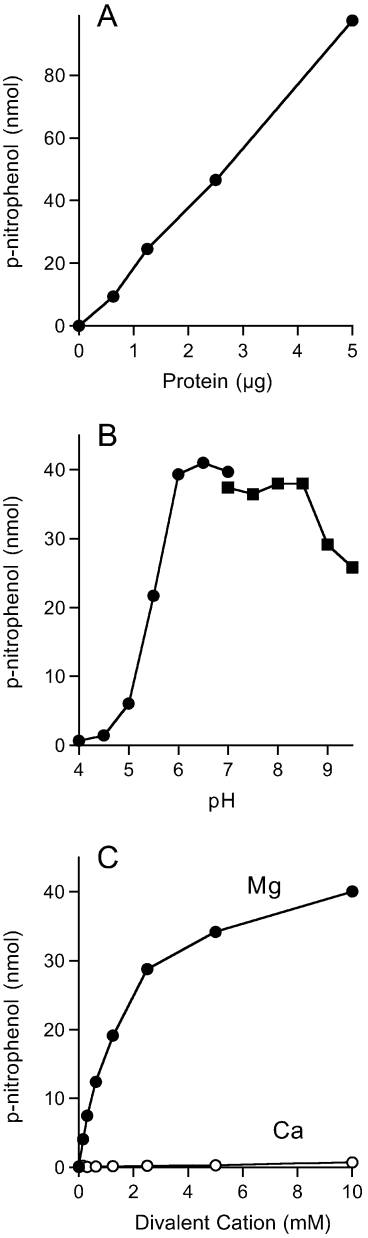

FIGURE 3: Phosphatase activity of recombinant EcFcp1. In panel A, reaction mixtures (200 μL) containing 50 mM Tris-acetate (pH 6.5), 10 mM $MgCl_2$, 10 mM pNØP, and His_{10}-Smt3-EcFcp1 as specified were incubated for 60 min at 37 °C. pNØ release is plotted as a function of input protein. Panel B shows pH dependence data. Reaction mixtures (200 μL) containing either 50 mM Tris-acetate (pH 4.0, 4.5, 5.0, 5.5, 6.0, 6.5, or 7.0; ●) or 50 mM Tris-HCl (pH 7.0, 7.5, 8.0, 8.5, 9.0, or 9.5; ■), 10 mM $MgCl_2$, 10 mM pNØP, and 2.5 μg of His_{10}-Smt3-EcFcp1 were incubated for 60 min at 37 °C. pNØ release is plotted as a function of pH. Panel C shows the divalent cation requirement. Reaction mixtures containing 50 mM Tris-acetate (pH 6.5), 10 mM pNØP, 2.5 μg of His_{10}-Smt3-EcFcp1, and either $MgCl_2$ or $CaCl_2$ as specified were incubated for 60 min at 37 °C. pNØ release is plotted as a function of divalent cation concentration.

whether it displays any preference for the position of phosphoserine within the CTD heptad, we employed synthetic 28-aa peptides consisting of four tandem heptad repeats phosphorylated exclusively at Ser2 or Ser5 of each heptad. Release of inorganic phosphate from the CTD was measured colorimetrically by the malachite green method. Reaction of Fcp1 with 25 μM of either the CTD Ser2-PO_4 peptide or Ser5-PO_4 peptide resulted in P_i release proportional to input

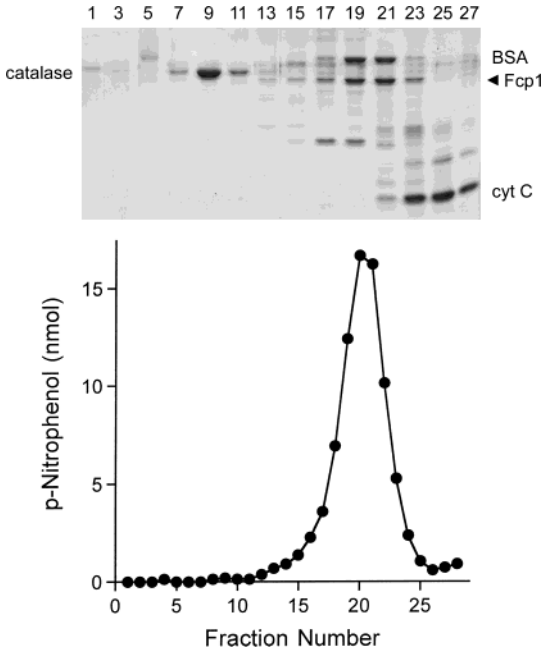

FIGURE 4: Glycerol gradient sedimentation. Sedimentation analysis was performed as described under Experimental Procedures. Aliquots (20 μL) of odd-numbered gradient fractions were analyzed by SDS−PAGE. The Coomassie Blue stained gel is shown (top panel) with the identities of the polypeptides indicated of on the left and right. The phosphatase activity profile is shown in the bottom panel.

His_{10}-Smt3-EcFcp1 (Figure 5A). Dephosphorylation of Ser5 and Ser2 reached a plateau at 2 μg of input protein, at which point 96% and 78% of the input Ser5-PO_4 and Ser2-PO_4 residues had been hydrolyzed, respectively. The specific activities for Ser5 and Ser2 phosphatase were 10 and 7.2 nmol of P_i release per microgram of protein in 60 min, respectively, which corresponds to turnover numbers of 0.16 and 0.11 s^{-1}. The instructive finding was that *E. cuniculi* Fcp1 did not display a significant position bias for Ser5 versus Ser2.

Phosphatase activity with the Ser5-PO_4 CTD peptide displayed a bell-shaped pH profile with an optimum at pH 7.0 (Figure 5B). CTD phosphatase activity was abolished at pH $\leq$ 5.0 or $\geq$ 9.0. CTD phosphatase activity required a divalent cation cofactor (Figure 5C). Magnesium supported optimal activity at 10 mM concentration. Manganese and cobalt (10 mM) were also capable of satisfying the divalent cation requirement, albeit less effectively than 10 mM magnesium. Calcium, copper, and zinc (10 mM) were ineffective as CTD phosphatase cofactors (Figure 5C).

EcFcp1 Dephosphorylates Only the Distal Phosphate in a Diheptad Ser2-PO_4 Substrate. The experiment in Figure 5A using a tetraheptad CTD Ser2-PO_4 substrate showed that 22% of the input Ser2-PO_4 was unreactive with EcFcp1 (i.e., only 78% of the available phosphate was hydrolyzed at saturating enzyme). To explain this result, we considered that EcFcp1 might require a minimal length CTD peptide flanking each Ser2-PO_4 and that either the N-terminal heptad or the C-terminal heptad of the 28-aa substrate lacks the requisite flanking amino acids. To address this issue, we exploited a 14-aa diheptad CTD peptide YSPTSPSYSPTSPS phosphorylated at Ser2 of each heptad. Reaction of His_{10}-Smt3-EcFcp1 with 100 μM of the diheptad Ser2-PO_4 CTD peptide resulted in P_i release proportional to the amount of

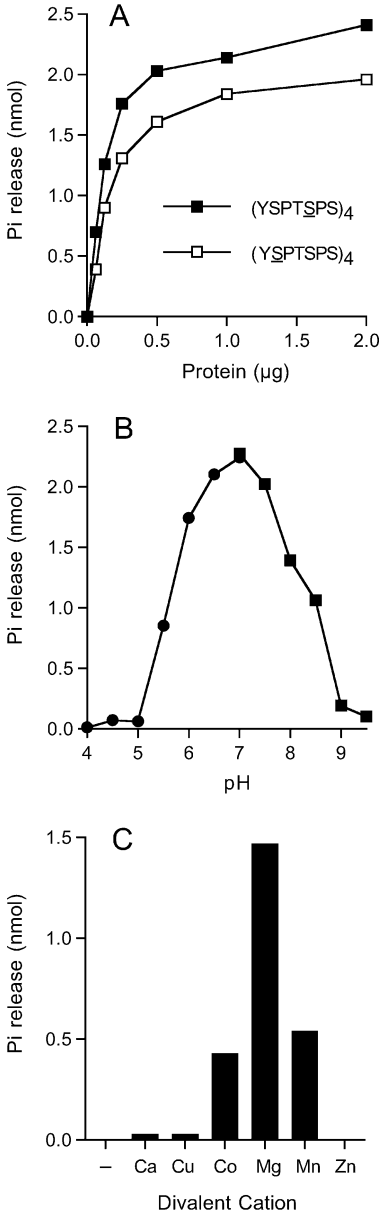

FIGURE 5: CTD phosphatase activity. In panel A, reaction mixtures (25 μL) containing 50 mM Tris-acetate (pH 6.5), 10 mM $MgCl_2$, either 25 μM $(YSPTSPS)_4$ or 25 μM $(YSPTSPS)_4$ peptide as indicated (corresponding to 100 μM Ser-PO_4), and His_{10}-Smt3-EcFcp1 as specified were incubated for 60 min at 37 °C. Phosphate release is plotted as a function of input protein. Panel B shows pH dependence data. Reaction mixtures (25 μL) containing either 50 mM Tris-acetate (pH 4.0, 4.5, 5.0, 5.5, 6.0, 6.5, or 7.0; ●) or 50 mM Tris-HCl (pH 7.0, 7.5, 8.0, 8.5, 9.0, or 9.5; ■), 10 mM $MgCl_2$, 25 μM $(YSPTSPS)_4$ peptide, and 0.2 μg of His_{10}-Smt3-EcFcp1 were incubated for 60 min at 37 °C. Phosphate release is plotted as a function of pH. Panel C shows the divalent cation specificity. Reaction mixtures containing 50 mM Tris-acetate (pH 7.0), 25 μM $(YSPTSPS)_4$ peptide, 0.125 μg of His_{10}-Smt3-EcFcp1, and either 10 mM divalent cation as specified (all as chloride salts) or no added divalent cation (−) were incubated for 60 min at 37 °C.

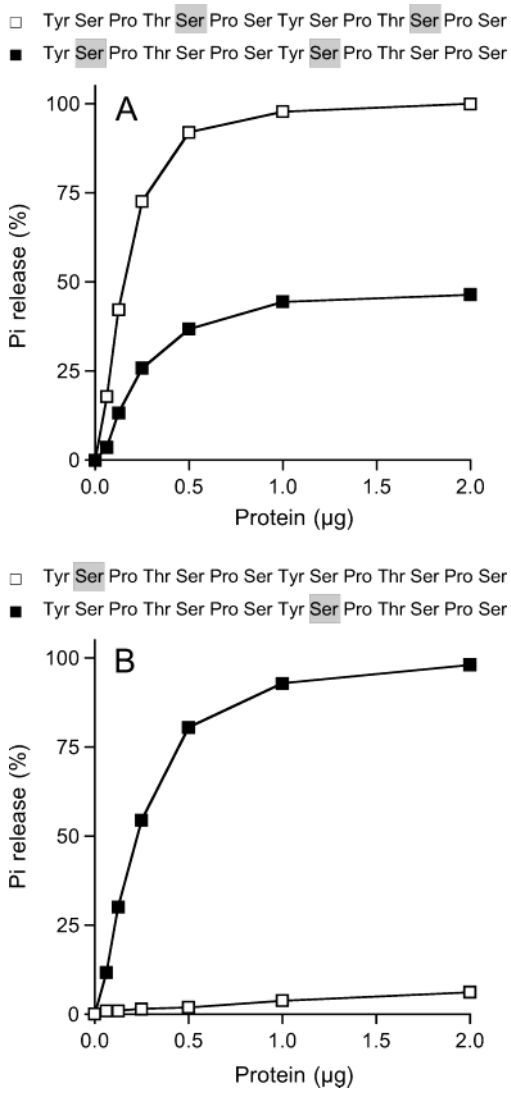

FIGURE 6: EcFcp1 dephosphorylates a phosphopeptide with two heptads repeats. In panel A, the sequences of the 14-aa CTD phosphopeptides are depicted with Ser5-PO_4 or Ser2-PO_4 positions highlighted in shaded boxes. Reaction mixtures (25 μL) containing 50 mM Tris-acetate (pH 7.0), 10 mM $MgCl_2$, 100 μM CTD peptide (corresponding to 200 μM Ser-PO_4), and His_{10}-Smt3-EcFcp1 as specified were incubated for 60 min at 37 °C. Activity is expressed as the percent of input Ser-PO_4 released as P_i. In panel B, the sequences of the diheptad CTD peptides containing a single Ser2-PO_4 in either the first heptad repeat or the second heptad repeat are shown. Reaction mixtures (25 μL) containing 50 mM Tris-acetate (pH 7.0), 10 mM $MgCl_2$, 100 μM CTD peptide, and His_{10}-Smt3-EcFcp1 as specified were incubated for 60 min at 37 °C. Activity is expressed as the percent of input Ser2-PO_4 released as P_i.

input enzyme (Figure 6A, titration curve ■); 46% of the input phosphoserine was hydrolyzed at saturating enzyme levels. Apparently, only one of the two available Ser2-PO_4 heptads served as a substrate for His_{10}-Smt3-EcFcp1. To determine which phosphoserine was dephosphorylated and which was resistant, we tested two 14-mer monophosphorylated CTD peptides, which contained Ser2-PO_4 in either the N-terminal heptad (YSPTSPSYSPTSPS) or the C-terminal heptad (YSPTSPSYSPTSPS). Reaction of His_{10}-Smt3-EcFcp1 with 100 μM of the YSPTSPSYSPTSPS peptide resulted in quantitative P_i release that was proportional to input enzyme (Figure 6B, titration curve ■). In contrast, His_{10}-Smt3-EcFcp1 was virtually unreactive with 100 μM of the YSPTSPSYSPTSPS peptide (Figure 6B, titration curve □). From the slopes of the titration curves, we calculated that EcFcp1 specific activity with the phosphorylated N-terminal heptad was 1.2% of the specific activity with the phosphorylated C-terminal heptad.

These experiments demonstrate that (i) a diheptad CTD peptide suffices for hydrolysis of Ser2-PO_4 by *E. cuniculi* Fcp1, (ii) a single Ser2-PO_4 residue suffices for activity,

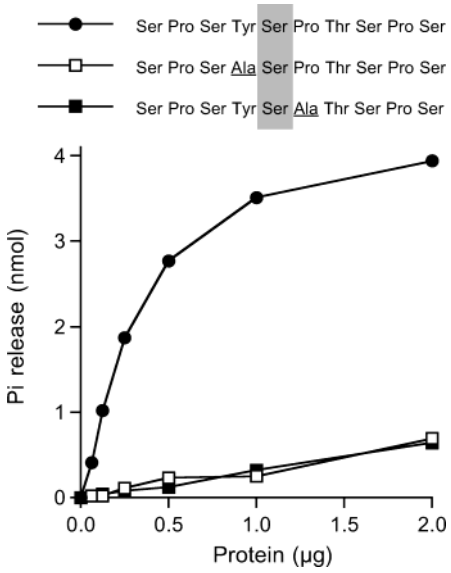

FIGURE 7: Tyr1 and Pro3 are critical for CTD Ser2 phosphatase activity. The wild-type and mutant 10-aa CTD phosphopeptides are depicted with Ser2-PO_4 positions highlighted in shaded boxes. The Y1A and P3A mutations are underlined. Reaction mixtures (25 μL) containing 50 mM Tris-acetate (pH 7.0), 10 mM $MgCl_2$, 160 μM CTD peptide, and His_{10}-Smt3-EcFcp1 as specified were incubated for 60 min at 37 °C. Phosphate release is plotted as a function of input protein.

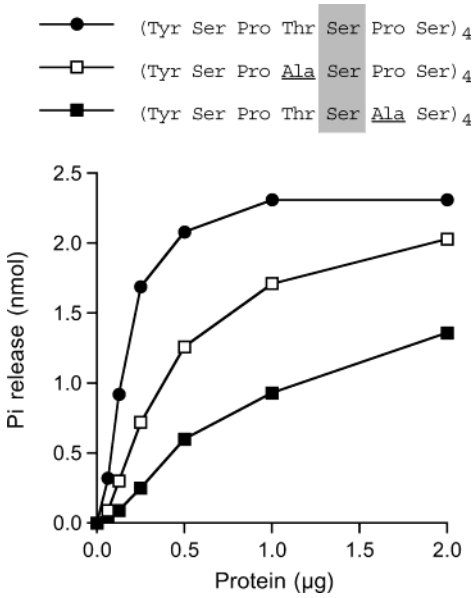

FIGURE 8: Effects of T4A and P6A mutations on CTD Ser5 phosphatase activity. The wild-type and mutated tetraheptad CTD phosphopeptides are depicted with Ser5-PO_4 positions highlighted in shaded boxes. The T4A and P6A mutations are underlined. Reaction mixtures (25 μL) containing 50 mM Tris-acetate (pH 7.0), 10 mM $MgCl_2$, 25 μM CTD peptide (corresponding to 100 μM Ser-PO_4), and His_{10}-Smt3-EcFcp1 as specified were incubated for 60 min at 37 °C. Phosphate release is plotted as a function of input protein.

provided that it is phased in the appropriate context with as few as five residues on the C-terminal side of the Ser2-PO_4, and (iii) Ser2-PO_4 cannot be hydrolyzed by *E. cuniculi* Fcp1 when only a single tyrosine residue is present on its N-terminal flank.

Minimal CTD Substrate and the Role of Tyr1 and Pro3 in Dephosphorylation of Ser2. His_{10}-Smt3-EcFcp1 catalyzed quantitative release of P_i from a 10-mer peptide SPSYSPTSPS containing 4-aa on the N-terminal side and 5-aa on the C-terminal side of Ser2-PO_4 (Figure 7). To investigate the role of the amino acid side chains flanking phosphoserine as determinants of EcFcp1 activity, we tested mutated versions of the 10-mer CTD phosphopeptide SPSYSPTSPS, wherein Tyr1 or Pro3 was replaced individually by alanine (Figure 7). The specific activities of His_{10}-Smt3-EcFcp1 with the Y1A (SPSASPTSPS) and P3A (SPSYSATSPS) substrates were 4.3% and 4.2%, respectively, of the activity with the wild-type CTD substrate.

EcFcp1 Dephosphorylates Both Phosphates in a Diheptad Ser5-PO_4 Substrate. Reaction of His_{10}-Smt3-EcFcp1 with 100 μM of a 14-aa diheptad CTD Ser5-PO_4 peptide YSPTSPSYSPTSPS resulted in P_i release proportional to the amount of input enzyme (Figure 6A). Both phosphates of the substrate were accessible to the enzyme, insofar as the input phosphoserine was hydrolyzed completely at saturating enzyme levels. This experiment shows that four consensus amino acids on the N-terminal side of the Ser5-PO_4 and two amino acids on the C-terminal side suffice for *E. cuniculi* Fcp1 CTD phosphatase activity.

Role of Thr4 and Pro6 in Dephosphorylation of Ser5. To probe the role of the Thr4 and Pro6 side chains flanking Ser5 as determinants of EcFcp1 activity, we tested mutated versions of the tetraheptad CTD Ser5-PO_4 peptide $(YSPTSPS)_4$, wherein Thr4 or Pro6 was replaced individually by alanine. The titration profiles of the reaction of His_{10}-Smt3-EcFcp1 with the T4A or P6A substrates displayed a shift to the right compared to the wild-type CTD peptide (Figure 8). The specific activities of His_{10}-Smt3-EcFcp1 with the T4A and P6A substrates were 44% and 14%, respectively, of the activity with the wild-type $(YSPTSPS)_4$ substrate.

EcFcp1 Can Replace S. cerevisiae Fcp1 In Vivo. EcFcp1 was tested for its ability to function in vivo in yeast in lieu of the essential *S. cerevisiae* CTD phosphatase Fcp1. The wild-type *EcFCP1* cDNA was cloned into a yeast 2μ *TRP1* plasmid vector so as to place its expression under the control of the constitutive *TPI1* promoter. Two mutated alleles, *EcFCP1-D66A* and *EcFCP1-D68A*, were also cloned into the 2μ *TRP1* vector; the D66A mutation in the signature DxDx(T/V) motif of EcFcp1 eliminates the aspartate nucleophile and abolishes the phosphatase activity of recombinant EcFcp1 (data not shown). The *EcFCP1* and *D66A* and *D68A* plasmids were transformed into a *S. cerevisiae fcp1*Δ strain in which the chromosomal *FCP1* gene was deleted and replaced by *LEU2*. Growth of *fcp1*Δ is contingent on maintenance of a wild-type *FCP1* allele on a *CEN URA3* plasmid. Control experiments showed that the *fcp1*Δ strain was unable to grow on agar medium containing 5-FOA (a drug that selects against the *URA3* plasmid) when transformed with an empty *TRP1* vector but readily yielded colonies on 5-FOA when transformed with a plasmid containing the wild-type *S. cerevisiae FCP1* gene. The instructive findings were that *fcp1*Δ cells transformed with a 2μ *TRP1 EcFCP1* plasmid formed colonies on 5-FOA agar, whereas cells transformed with the *EcFCP1-D66A* or *EcFCP1-D68A* mutant did not (not shown). Thus, EcFcp1 is a genuine ortholog of yeast Fcp1, and its ability to sustain cell growth depends on its phosphatase activity. To our knowledge, this is the first example in which a heterologous

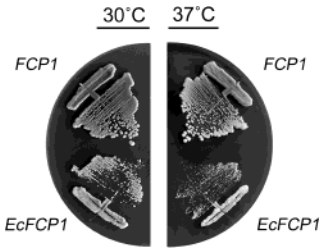

FIGURE 9: EcFcp1 functions in vivo in lieu of *S. cerevisiae* Fcp1. EcFcp1 activity in vivo in a yeast *fcp1*Δ strain was tested by plasmid shuffle as described under Experimental Procedures. Individual FOA-resistant *fcp1*Δ *FCP1* and *fcp1*Δ *EcFCP1* isolates were streaked on YPD agar. The plates were photographed after incubation for 4 days at 30 or 37 °C.

CTD phosphatase has been shown to function in vivo in yeast.

We noted that the *fcp1*Δ *2μ EcFCP1* yeast strain formed smaller colonies than did an isogenic *FCP1* strain when grown in a parallel on rich medium (YPD agar) at 25, 30, and 37 °C (Figure 9 and data not shown), suggesting that whereas EcFcp1 suffices for cell viability, it may not perform as well as the endogenous yeast Fcp1, either because of inherent functional distinctions between the yeast and microsporidian CTD phosphatases or because EcFcp1 function in yeast is limited by protein expression. Consistent with either idea, we found that *EcFCP1* complementation of *fcp1*Δ requires high gene dosage, that is, *fcp1*Δ cells transformed with *EcFCP1* on a single-copy *CEN* plasmid under the control of the constitutive *TPI1* promoter were unable to grow on 5-FOA (not shown).

DISCUSSION

The present study advances on several fronts our knowledge of the enzymology of CTD phosphatases by (i) identifying a minimized Fcp1 homologue in the microsporidian parasite *E. cuniculi* and documenting its intrinsic activity in dephosphorylating CTD positions Ser2 and Ser5 with similar efficacy in vitro, (ii) demonstrating genetically that *E. cuniculi* Fcp1 is a genuine ortholog of *S. cerevisiae* Fcp1, (iii) defining minimized CTD Ser2-PO_4 and Ser5-PO_4 peptide substrates for EcFcp1, and (iv) illuminating the role of CTD primary structure as a determinant of CTD phosphatase activity.

Early work showed that the activity of yeast and human Fcp1 in dephosphorylating Pol II was stimulated by transcription factor TFIIF (*19, 35*). Human Fcp1 dephosphorylates either Ser2 or Ser5 of the native Pol II CTD in the presence of TFIIF but does not dephosphorylate CTD-PO_4 separated from the body of Pol II (*15, 36*). Our studies have focused on the intrinsic catalytic properties and specificities of Fcp1 enzymes from two unicellular eukarya: *Sc. pombe* and *E. cuniculi*. Unlike human Fcp1, both SpFcp1 and EcFcp1 display comparatively vigorous phosphatase activities per se (as recombinant proteins produced in bacteria) with either pNØP or synthetic CTD phosphopeptide substrates. We have used synthetic CTD phosphopeptides to illuminate in detail the inherent 6- to 10-fold preference of *Sc. pombe* Fcp1 for dephosphorylation of Ser2 of the $Y^1S^2P^3T^4S^5P^6S^7$ heptad compared to its activity in dephosphorylating Ser5 (*27, 32*). In contrast, we find here that *E. cuniculi* Fcp1 dephosphorylates both Ser5 and Ser2, with a slight preference for Ser5. A recently identified family of human small CTD phosphatases (SCPs) is also able to dephosphorylate synthetic tetraheptad CTD phosphopeptides with a slight preference for the Ser5-PO_4 substrate versus Ser2-PO_4 (*15*). These findings underscore the point that Fcp1 or Fcp1-like CTD phosphatases from different species, or even paralogous CTD phosphatases from the same species (*15, 16*), cannot be presumed to have the same inherent biochemical properties and substrate specificities.

A biochemical property that varies from one Fcp1 enzyme to another is the dependence of phosphatase activity on pH. As shown here, *E. cuniculi* Fcp1 displays a neutral pH optimum in its hydrolysis of pNØP or CTD-PO_4 substrates and is poorly active with either substrate at pH $\leq$ 5.0. (Human Fcp1 behaves similarly in dephosphorylating Pol II (*36*).) This pH profile contrasts sharply with that of *Sc. pombe* Fcp1, which is optimally active at pH 5.5 with either pNØP or CTD-PO_4 substrates (*27*), and with human SCP1, which has optimal phosphatase activity at pH 4.0−5.0 (*15*). As we discussed previously (*29*), it is sensible that Fcp1, as a DxDx(T/V) phosphatase, would display optimal activity at mildly acidic pH, because the phosphoryl transfer mechanism calls for an unprotonated aspartate nucleophile and a protonated aspartate general acid catalyst. An alkaline shift in the pH optimum of some Fcp1 enzymes can be explained if (i) the electrostatic environment at the active site increases the pK_a of one or both of the catalytic aspartates or (ii) the observed phosphatase activity is subject to a rate-limiting step other than phosphoryl transfer chemistry.

The reported degrees of stimulation of various DxDx(T/V)-type CTD phosphatases by TFIIF or the isolated TFIIF large subunit are in the range of 5- to 10-fold (*15, 35*). Recent studies suggest that binding of human Fcp1 to TFIIF and stimulation of Fcp1 phosphatase activity depends on covalent modification of Fcp1 by phosphorylation (*37, 38*). A discrete α-helical C-terminal 18-aa segment of human Fcp1 mediates its binding to TFIIF (*21, 39*). The 411-aa *E. cuniculi* Fcp1 protein lacks the large polypeptide segments found upstream of the FCPH domain and downstream of the BRCT domain of the metazoan and fungal Fcp1 proteins, but it retains a short C-terminal peptide CDHRTKDEYEEELERLF^{410} that bears noteworthy similarity to the C-terminal TFIIF-binding motif of human Fcp1 EADEMAKALEAELNDLM (conserved positions are underlined). Thus, it is possible that EcFcp1 exploits this peptide to interact with the (as yet uncharacterized) *E. cuniculi* homologue of TFIIF.

Our finding that EcFcp1 can sustain yeast cell growth in lieu of *S. cerevisiae* Fcp1 is, to our knowledge, the first instance of cross-species complementation of Fcp1 function in vivo. The fact that a minimal Fcp1 ortholog consisting only of the core catalytic domain (and perhaps a short TFIIF-binding peptide) can function in vivo is relevant in light of earlier deletion analyses of *S. cerevisiae* Fcp1, which showed that removal of the N-terminal region upstream of the Fcp1-homology domain did not affect cell viability, nor did removal of the C-terminal segment downstream of the BRCT domain (including the C-terminal TFIIF-binding site), but simultaneous deletion of both N- and C-terminal segments was lethal in vivo (*30*). It would appear that budding yeast has embellished the minimal Fcp1 core with additional (and functionally redundant) flanking domains. The extra N- and C-terminal domains may serve ancillary noncatalytic func-

tions attributed to Fcp1, such as stimulation of Pol II elongation (*22*, *40*).

The present analysis of the hydrolysis by *E. cuniculi* Fcp1 of synthetic CTD phosphopeptides illuminates the contributions of CTD length, heptad phasing, and individual conserved CTD side chains to its CTD Ser2 and Ser5 phosphatase activities. We have shown that (i) a properly phased decapeptide $S^5P^6S^7Y^1\underline{S}^2P^3T^4S^{5'}P^{6'}S^{7'}$ suffices for efficient Ser2 phosphatase activity in vitro, (ii) a single tyrosine residue upstream of Ser2-PO_4 does not suffice, and (iii) the Tyr1 and Pro3 side chains flanking the phosphoserine are critical features of the substrate, that is, their single replacement by alanine reduces activity by a factor of 25. These properties of EcFcp1 generally echo those of the Ser2 phosphatase of *Sc. pombe* Fcp1 (*32*).

EcFcp1 quantitatively removed two Ser5 phosphates from a diheptad CTD phosphopeptide, indicating that as few as four amino acids upstream and two amino acids downstream of Ser5-PO_4 position suffice for activity. Replacement of Pro6 by alanine reduced Ser5 phosphatase activity by a factor of 7. Together, the effects of the P3A and P6A mutations on the Ser2 and Ser5 phosphatase activities show that EcFcp1 is a proline-directed protein serine phosphatase. Loss of the Thr4 side chain has relatively little impact on the Ser5 phosphatase activity of EcFcp1, despite the fact that a threonine side chain is present at position 4 in all 15 repeats of the *E. cuniculi* Pol II CTD. Yet, the result is consistent with the fact that *S. cerevisiae* is viable when every one of the Thr4 positions in its CTD is replaced by alanine (*41*). It is therefore likely that EcFcp1 relies on features other than the side chain at position 4 to effectively bind and hydrolyze Ser5-PO_4.

REFERENCES

1. Bartolomei, M. S., Halden, N. F., Cullen, C. R., and Corden, J. L. (1988) Genetic analysis of the repetitive carboxyl-terminal domain of the largest subunit of RNA polymerase II, *Mol. Cell. Biol. 8*, 330−339.
2. Zehring, W. A., Lee, J. M., Weeks, J. R., Jokerst, R. S., and Greenleaf, A. L. (1988) The C-terminal repeat domain of RNA polymerase II largest subunit is essential in vivo but is not required for accurate transcription initiation in vitro, *Proc. Natl. Acad. Sci. U.S.A. 85*, 3698−3702.
3. Nonet, M., Sweetser, D., and Young, R. A. (1987) Functional redundancy and structural polymorphism in the large subunit of RNA polymerase II, *Cell 50*, 909−915.
4. West, M. L., and Corden, J. L. (1995) Construction and analysis of yeast RNA polymerase II CTD deletion and substitution mutations, *Genetics 140*, 1223−1233.
5. Katinka, M. D., Duprat, S., Cornillot, E., Méténier, G., Thormarat, F., Prensier, G., Barbe, V., Peyretaillade, E., Brottier, P., Wincker, P., Delbac, F., El Alaoui, H. Peyret, P., Saurin, W., Gouy, M., Weissenbach, J., and Vivarès, C. P. (2001) Genome sequence and gene compaction of the eukaryote parasite *Encephalitozoon cuniculi*, *Nature 414*, 450−453.
6. Kobor, M. S., and Greenblatt, J. (2002) Regulation of transcription elongation by phosphorylation, *Biochim. Biophys. Acta 1577*, 261−275.
7. Lin, P. S., Marshall, N. F., and Dahmus, M. E. (2002) CTD phosphatase: role in RNA polymerase II cycling and the regulation of transcript elongation, *Prog. Nucleic Acid Res. Mol. Biol. 72*, 333−365.
8. Bentley, D. (2002) The mRNA assembly line: transcription and processing machines in the same factory, *Curr. Opin. Cell Biol.* 14, 336−342.
9. Ho, C. K., and Shuman, S. (1999) Distinct roles for CTD Ser2 and Ser5 phosphorylation in the recruitment and allosteric activation of mammalian capping enzyme, *Mol. Cell 3*, 405−411.
10. Pei, Y., Hausmann, S., Ho, C. K., Schwer, B., and Shuman, S. (2001) The length, phosphorylation state, and primary structure of the RNA polymerase II carboxyl-terminal domain dictate interactions with mRNA capping enzymes, *J. Biol. Chem. 276*, 28075−28082.
11. Fabrega, C., Shen, V., Shuman, S., and Lima, C. D. (2003) Structure of an mRNA capping enzyme bound to the phosphorylated carboxyl-terminal domain of RNA polymerase II, *Mol. Cell 11*, 1549−1561.
12. Hausmann, S., Vivarès, C. P., and Shuman, S. (2002) Characterization of the mRNA capping apparatus of the microsporidian parasite *Encephalitozoon cuniculi*, *J. Biol. Chem. 277*, 96−103.
13. Fabrega, C., Hausmann, S., Shen, V., Shuman, S., and Lima, C. D. (2004) Structure and mechanism of cap (guanine-N7) methyltransferase, *Mol. Cell 13*, 77−89.
14. Prelich, G. (2002) RNA polymerase II carboxyl-terminal domain kinases: emerging clues to their function, *Eukaryotic Cell 1*, 153−162.
15. Yeo, M., Patrick, P. S., Dahmus, M. E., and Gill, G. N. (2003) A novel RNA polymerase II C-terminal domain phosphatase that preferentially dephosphorylates serine 5, *J. Biol. Chem. 278*, 26078−26085.
16. Koiwa, H., Barb, A. W., Xiong, L., Li, F., McCully, M. G., Lee, B., Sokolchik, I., Zhu, J., Gong, Z., Reddy, M., Sharkhuu, A., Manabe, Y., Yokoi, S., Zhu, J. K., Bressan, R. A., and Hasegawa, P. M. (2002) C-terminal domain phosphatase-like family members (AtCPLs) differentially regulate *Arabidopsis thaliana* abiotic stress signaling, growth, and development, *Proc. Natl. Acad. Sci. U.S.A. 99*, 10893−10898.
17. Washington, K., Ammosova, T., Beullens, M., Jerebtsova, M., Kumar, A., Bollen, M., and Nekhai, S. (2002) Protein phosphatase-1 dephosphorylates the C-terminal domain of RNA polymerase II, *J. Biol. Chem. 277*, 40442−40448.
18. Chambers, R. S., and Dahmus, M. E. (1994) Purification and characterization of a phosphatase from HeLa cells which dephosphorylates the C-terminal domain of RNA polymerase II, *J. Biol. Chem. 269*, 26243−26248.
19. Chambers, R. S., and Kane, C. M. (1996) Purification and characterization of an RNA polymerase II phosphatase from yeast, *J. Biol Chem. 271*, 24498−24504.
20. Archambault, J., Chambers, R. S., Kobor, M. S., Ho, Y., Cartier, M., Bolotin, D., Andrews, B., Kane, C. M., and Greenblatt, J. (1997) An essential component of a C-terminal domain phosphatase that interacts with transcription factor IIF in *Saccharomyces cerevisiae*, *Proc. Natl. Acad. Sci. U.S.A. 94*, 14300−14305.
21. Archambault, J., Pan, G., Dahmus, G. K., Cartier, M., Marshall, N., Zhang, S., Dahmus, M. E., and Greenblatt, J. (1998) FCP1, the RAP74-interacting subunit of a human protein phosphatase that dephosphorylates the carboxyl-terminal domain of RNA polymerase IIO, *J. Biol. Chem. 273*, 27593−27601.
22. Cho, H., Kim, T., Mancebo, H., Lane, W. S., Flores, O., and Reinberg, D. (1999) A protein phosphatase functions to recycle RNA polymerase II, *Genes Dev. 13*, 1540−1552.
23. Kobor, M. S., Archambault, J., Lester, W., Holstege, F. C. P., Gileadi, O., Lansma, D. B., Jennings, E. G., Kouyoumdjian, F., Davidson, A. R., Young, R. A., and Greenblatt, J. (1999) A unusual eukaryotic protein phosphatase required for transcription by RNA polymerase II and CTD dephosphorylation in *S. cerevisiae*, *Mol. Cell 4*, 55−62.
24. Palancade, B., Dubois, M. F., Dahmus, M. E., and Bensaude, O. (2001) Transcription-independent RNA polymerase II dephosphorylation by the FCP1 carboxyl-terminal domain phosphatase in *Xenopus laevis* early embryos, *Mol. Cell. Biol. 21* 6359−6368.
25. Cho, E. J., Kobor, M. S., Kim, M., Greenblatt, J., and Buratowski, S. (2001) Opposing effects of Ctk1 kinase and Fcp1 phosphatase at Ser2 of the RNA polymerase II C-terminal domain, *Genes Dev. 15*, 3319−3329.
26. Kimura, M., Suzuki, H., and Ishihama, A. (2002) Formation of a carboxyl-terminal phosphatase (Fcp1)/TFIIF/RNA polymerase II (pol II) complex in *Schizosaccharomyces pombe* involves direct interaction between Fcp1 and the Rpb4 subunit of pol II, *Mol. Cell. Biol. 22*, 1577−1588.
27. Hausmann, S., and Shuman, S. (2002) Characterization of the CTD phosphatase Fcp1 from fission yeast: preferential dephosphorylation of serine 2 versus serine 5, *J. Biol. Chem. 277*, 21213−21220.

28. Varon, R., Gooding, R., Steglich, C., Marns, L., Tang, H., Angelicheva, D., Yong, K. K., Ambrugger, P., Reinhold, A., Morar, B., Baas, F., Kwa, M., Tournev, I., Guerguelcheva, V., Kremensky, I., Lochmüller, H., Müllner-Eidenböck, A., Merlini, L., Neumann, L., Bürger, J., Wallter, M., Swoboda, K., Thomas, P. K., von Moers, A., Risch, N., and Kalaydjieva, L. (2003) Partial deficiency of the C-terminal-domain phosphatase of RNA polymerase II is associated with congenital cataracts facial dysmorphism neuropathy syndrome, *Nat. Genet. 35*, 185−189.
29. Hausmann, S., and Shuman, S. (2003) Defining the active site of *Schizosaccharomyces pombe* CTD phosphatase Fcp1, *J. Biol. Chem. 278*, 13627−13632.
30. Kobor, M. S., Simon, L. D., Omichinski, J., Zhong, G., Archambault, J., and Greenblatt, J. (2000) A motif shared by TFIIF and TFIIB mediates their interaction with the RNA polymerase II carboxyl-terminal domain phosphatase Fcp1p in *Saccharomyces cerevisiae*, *Mol. Cell. Biol. 20*, 7438−7449.
31. Collet, J. F., Stroobant, V., Pirard, M., Delpierre, G., and Van Schaftingen, E. (1998) A new class of phosphotransferases phosphorylated on an aspartate residue in an amino-terminal D*X*D*X*(T/V) motif, *J. Biol. Chem. 273*, 14107−14112.
32. Hausmann, S., Erdjument-Bromage, H., and Shuman, S. (2004) *Schizosaccharomyces pombe* carboxyl-terminal domain (CTD) phosphatase Fcp1: distributive mechanism, minimal CTD substrate, and active site mapping, *J. Biol. Chem. 279*, 10892−10900.
33. Yu, X., Chini, C. C. S, He, M., Mer, G., and Chen, J. (2003) The BRCT domain is a phospho-protein binding domain, *Science 302*, 639−642.
34. Mossessova, E., and Lima, C. D. (2000) Ulp1-SUMO crystal structure and genetic analysis reveal conserved interactions and a regulatory element essential for cell growth in yeast, *Mol. Cell 5*, 865−876.
35. Chambers, R. S., Wang, B. Q., Burton, Z. F., and Dahmus, M. E. (1995) The activity of COOH-terminal domain phosphatase is regulated by a docking site on RNA polymerase II and by the general transcription factors IIF and IIB, *J. Biol. Chem. 270*, 14962−14969.
36. Lin, P. S., Dubois, M. F., and Dahmus, M. E. (2002) TFIIF-associating carboxyl-terminal domain phosphatase dephosphorylates phosphoserines 2 and 5 of RNA polymerase II, *J. Biol. Chem. 277*, 45949−45946.
37. Friedl, E. M., Lane, W. S., Erdjument-Bromage, H., Tempst, P., and Reinberg, D. (2003) The C-terminal domain phosphatase and transcription elongation activities of FCP1 are regulated by phosphorylation, *Proc. Natl. Acad. Sci. U.S.A. 100*, 2328−2333.
38. Palancade, B., Dubois, M. F., and Bensaude, O. (2002) FCP1 phosphorylation by casein kinase 2 enhances binding to TFIIF and RNA polymerase II carboxyl-terminal domain phosphatase activity, *J. Biol. Chem. 277*, 36061−36067.
39. Kamada, K., Roeder, R. G., and Burley, S. K. (2003) Molecular mechanism of recruitment of TFIIF-associating RNA polymerase C-terminal domain phosphatase (FCP1) by transcription factor IIF, *Proc. Natl. Acad. Sci. U.S.A. 100*, 2296−2299.
40. Mandal, S. S., Cho, H., Kim, S., Cabane, K., and Reinberg, D. (2002) FCP1, a phosphatase specific for the heptapeptide repeat of the largest subunit of RNA polymerase II, stimulates transcription elongation, *Mol. Cell. Biol. 22*, 7543−7552.
41. Stiller, J. W., McConaughy, B. L., and Hall, B. D. (2000) Evolutionary complementation for polymerase II CTD function, *Yeast 16*, 57−64.

BI0499617